energies

MDPI

Article

A Carbide Slag-Based, $Ca_{12}Al_{14}O_{33}$-Stabilized Sorbent Prepared by the Hydrothermal Template Method Enabling Efficient CO_2 Capture

Xiaotong Ma [1], Yingjie Li [1,*], Yi Qian [1] and Zeyan Wang [2]

[1] School of Energy and Power Engineering, Shandong University, Jinan 250061, China
[2] State Key Laboratory of Crystal Materials, Shandong University, Jinan 250100, China
* Correspondence: liyj@sdu.edu.cn; Tel.: +86-0531-883-92414

Received: 25 May 2019; Accepted: 4 July 2019; Published: 8 July 2019

Abstract: Calcium looping is a promising technology to capture CO_2 from the process of coal-fired power generation and gasification of coal/biomass for hydrogen production. The decay of CO_2 capture activities of calcium-based sorbents is one of the main problems holding back the development of the technology. Taking carbide slag as a main raw material and $Ca_{12}Al_{14}O_{33}$ as a support, highly active CO_2 sorbents were prepared using the hydrothermal template method in this work. The effects of support ratio, cycle number, and reaction conditions were evaluated. The results show that $Ca_{12}Al_{14}O_{33}$ generated effectively improves the cyclic stability of CO_2 capture by synthetic sorbents. When the Al_2O_3 addition is 5%, or the $Ca_{12}Al_{14}O_{33}$ content is 10%, the synthetic sorbent possesses the highest cyclic CO_2 capture performance. Under harsh calcination conditions, the CO_2 capture capacity of the synthetic sorbent after 30 cycles is 0.29 g/g, which is 80% higher than that of carbide slag. The superiority of the synthetic sorbent on the CO_2 capture kinetics mainly reflects at the diffusion-controlled stage. The cumulative pore volume of the synthetic sorbent within the range of 10–100 nm is 2.4 times as high as that of calcined carbide slag. The structure of the synthetic sorbent reduces the CO_2 diffusion resistance, and thus leads to better CO_2 capture performance and reaction rate.

Keywords: carbide slag; calcium aluminates; calcium looping; CO_2 capture

1. Introduction

With the frequent occurrence of various extreme climates around the world and the increasingly intensified global climate change caused by greenhouse gases, a global consensus has been reached to reduce greenhouse gas emissions [1–3]. The *Special Report on Global Warming of 1.5 °C* adopted by the 48th plenary session of the Intergovernmental Panel on Climate Change (IPCC) [4] illustrates the point that human factors have caused global average temperature to increase by 1 °C compared with those before industrialization. If this trend continues, the global temperature could reach 1.5 °C or even 2 °C above the baseline, that is, pre-industrial level, sometime between 2030 and 2052. The main reason is that humans have been using fossil fuels (such as coal, oil, and so on) in large quantities, and the combustion process accompanied by heavy emissions of CO_2 and other greenhouse gases. Calcium looping (CaL) process is one of the feasible large-scale CO_2 capture technologies at present, which is applicable to the process of coal-fired power generation and gasification of coal/biomass for hydrogen production [5–9]. However, one of the problems restricting the development of this technology is the attenuation of CO_2 capture activity of CaO-based sorbents due to high-temperature sintering [10–12].

So far, how to improve the CO_2 capture performance of CaO-based sorbents has become a research hotspot. Researchers have put forward many methods to solve this problem, aiming

at optimizing CaO-based sorbents to maintain good CO_2 absorption activity and anti-sintering performance in the cyclic process, and finally obtaining a high CO_2 capture efficiency. These methods include hydration [13,14], thermal pre-treatment [15,16], use of porous CaO-based precursors [17,18], and doping [19–22]. Unfortunately, the modified sorbents still suffer from a pore blocking in the microstructure. Therefore, some inert materials serving as microstructure stabilizers have been added in the CaO-based sorbents [5,23–26].

Studies have shown that calcium aluminates can effectively stabilize the pore structure of CaO and retard the sintering of CaO particles [27–29]. CaO-based, calcium aluminates-stabilized sorbents have gained increasing interest owing to their advantages such as wide material sources, good sintering resistance, and high cyclic CO_2 capture capacity. The formation of calcium aluminates depended on different synthesis conditions and precursors. Zhou et al. [30] found that by means of mixing calcium nitrate and aluminum nitrate, CaO was uniformly mixed with $Ca_9Al_6O_{18}$, an inert support. Li et al. [31] proved that the uniform distribution of Ca, Al, and O atoms in the CaO/$Ca_3Al_2O_6$ composite sorbent was the main reason for the high CO_2 capture capacity of the sorbent. Vanga et al. [5] assessed a CaO/$Ca_{12}Al_{14}O_{33}$ sorbent over 200 multiple cycles and the stabilizing role of spacer $Ca_{12}Al_{14}O_{33}$ ceramic against sorbent decay was confirmed. Its CO_2 capture capacity drops by 13% up to 200 cycles. Rui et al. [24] reported that $Ca_3Al_2O_6$ was formed in the synthetic sorbent with the addition of 10 mol% Al_2O_3. The CO_2 capture capacity of the synthetic sorbent exceeded that of the benchmark CaO by more than 300% after 20 cycles. In addition, some low-cost industrial products or natural minerals, such as fly ash [32], attapulgite [33], kaolin [34,35], and cement [36–38], were also used to prepare CaO-based, calcium aluminates-stabilized sorbents. Chen et al. [32] found that doping fly ash into limestone could significantly improve the CO_2 capture performance of limestone, and $Ca_{12}Al_{14}O_{33}$ was generated as the support. After 20 cycles, the CO_2 absorption amount of the sorbent doped with fly ash was twice that of undoped limestone. Chen et al. [33] modified limestone by attapulgite using the wet mixing method, and the obtained $Ca_3Al_{10}O_{18}$ promoted the anti-sintering performance of the sorbents at a high temperature. The sorbent doped with 15 wt.% attapulgite displayed better CO_2 capture performance than limestone by an increase of 128% after 20 cycles under the same condition (calcination at 950 °C in 100% CO_2 and carbonation at 700 °C in 15% CO_2/85% N_2). Ridha et al. [34] used kaolin as both an aluminum source and a binder to granulate limestone. After 10 cycles under the calcination condition of 920 °C and pure CO_2, the carbonation conversion was 17%. Luo et al. [36] obtained a CaO/$Ca_{12}Al_{14}O_{33}$ sorbent by mixing sol-gel CaO powder with cement, which proved that the presence of $Ca_{12}Al_{14}O_{33}$ improved the CO_2 capture performance and cycling stability of the synthetic sorbent. At the carbonation and calcination temperatures of 650 °C and 850 °C, respectively, the CO_2 capture capacity after 50 cycles reached 0.43 g/g. Sun et al. [37] prepared pellets from limestone, cement, and rice husks via blending and pelletizing, which had a high CO_2 capture capacity and mechanical strength.

A large amount of carbide slag, mainly composed of $Ca(OH)_2$, is discharged from the polyvinyl chloride (PVC) and chlor-alkali industries every year [39,40]. In China, the annual output of PVC in a chlor-alkali plant is about 600,000 tons, accompanied by about 1.1 million tons of carbide slag generated per year [41]. In 2016, PVC production capacity reached 23 million tons in China, accounting for 40% of the global production capacity. This means that carbide slag output is more than 40 million tons a year. The piled-up carbide slag causes damage to the surrounding ecological environment and threatens human health. In addition, it is difficult to recycle carbide slag on a large scale, which results in the waste of calcium resources. Therefore, the utilization of carbide slag as CO_2 sorbents is supposed to solve the practical problem of waste accumulation and lower the cost of the CaL process.

It has been proven that carbon templating is a feasible way to synthesize ordered mesoporous CO_2 sorbents. Also, past work involved testing the sorbents prepared using carbide slag and alumina cement with the carbon template obtained from the hydrothermal carbonation of glucose. Although the synthetic sorbent showed stable CO_2 capture performance, its initial CO_2 uptake was low. It is necessary to study the method to further improve the CO_2 uptake. Li et al. [42] found that the limestone

treated with acetic acid solution had high CO_2 capture activity, and the carbonation conversion after 20 cycles was three times higher than that of untreated limestone. With the treatment by acetic acid, carbide slag with poor solubility in water can be converted into calcium acetate as a soluble material. It is generally known that soluble precursors are favorable for the homogenous distribution of CaO and inert supports, which is supposed to enhance the sintering resistance of CaO-based sorbents [30,31]. In addition, the pore structure of sorbents can be further improved to help increase the initial CO_2 uptake.

In this work, the synthetic sorbent with acid-washed carbide slag and aluminum nitrate as precursors by hydrothermal template method was reported. The CO_2 capture characteristics of synthetic sorbents were studied to validate the practical ability. Morphological characterizations were also used to explain the relationship between the micro pore structure and the performance.

2. Experimental

2.1. Sorbent Preparation

The carbide slag was sampled from a chlor-alkali plant in Shandong Province, China. The chemical components of the raw carbide slag were analyzed by X-ray fluorescence (XRF), as shown in Table 1. Aluminum nitrate, acetic acid, and glucose used in this work were analytical reagents.

Table 1. Chemical components of raw carbide slag (wt.%).

CaO	MgO	SiO_2	Al_2O_3	Fe_2O_3	SrO	Ti_2O	Others	Loss on Ignition
69.52	0.02	2.34	1.52	0.17	0.03	0.03	0.57	25.80

The template synthesis procedure was the same as in the previous work [43]. Aluminum nitrate was used as the aluminum precursor, acetic acid-washed carbide slag was used as the Ca precursor, and glucose was used as the carbon template precursor for template synthesis in this work. The acid-washing process of carbide slag was described below. Predetermined amounts of carbide slag were placed into a beaker. Deionized water was added at a carbide slag to deionized water ratio of 1 g/8 mL and the suspension was stirred evenly. Acetic acid was poured slowly into the suspension at a molar ratio of Ca to acetic acid of 2:1, and then it was stirred in a water bath at 50 °C for 20 min. The mixture was filtered and the filtrate was dried at 120 °C until all solids were separated. After grinding, the acetic acid-washed carbide slag was obtained. Synthetic sorbents were prepared by the hydrothermal template method. Glucose was dissolved in 60 mL deionized water to obtain a solution with a concentration of 1 mol/L. Six grams of acetic-washed carbide slag and aluminum nitrate with different CaO/Al_2O_3 weight ratios (97.5:2.5, 95:5, 92.5:7.5, and 90:10) were added to the solution and stirred in a water bath at 60 °C for 30 min. The mixture was poured into a high-pressure kettle for a hydrothermal synthesis at 180 °C for 6 h. The precipitate was collected after separation, washed with water and ethanol, dried, and pyrolyzed under a nitrogen flow at 450 °C for 2 h with a heating rate of 3 °C/min. Finally, the sample obtained was calcined under air at 600 °C for 1 h in a muffle furnace. It is worth noting that the errors of the CaO/Al_2O_3 ratios are less than 0.2%, considering that the complexity exists in carbide slag and the insoluble matter is removed during the acid-washing process. The synthetic sorbents were symbolized by HTx, where x is the weight percentage of Al_2O_3. As a comparison, the acetic acid-washed carbide slag and aluminum nitrate were directly mixed in a solution phase, dried, and calcined in air atmosphere at 600 °C for 1 h. The synthetic sorbent with the Al_2O_3 content of 5% was prepared by the wet mixing method, which is denoted as WM5. Weighed amounts of acetic acid-washed carbide slag and aluminum nitrate were mixed in a glass beaker. Water was added with stirring and the solution obtained was then pre-calcined under air at 600 °C for 1 h.

2.2. Cyclic CO_2 Capture Test

The cyclic calcination/carbonation reaction was performed in a dual fixed-bed reactor (DFBR) with a steam generator, as shown in Figure 1. The two reactors were a calciner and a carbonator, respectively. About 200 mg of the sample was placed into the calciner and maintained for 10 min for the full decomposition of the sample. Subsequently, the sample was cooled for 2.5 min in N_2 and weighed by a precise Mettler Toledo-XS105DU electronic balance (±0.1 mg). The sample was placed in the carbonator and maintained at 700 °C for 20 min. The weight of the sample after the carbonation was also measured, after which the calcination/carbonation cycles began. The preliminary experiments on the discontinuous 30 cycles of calcination/carbonation with cooling steps and continuous 10, 20, and 30 cycles without cooling steps were performed using carbide slag, respectively. The results showed that the cooling steps had a small impact on the CO_2 capture performance obtained, as shown in Figure 2. Therefore, masses of the sample were measured after each step in the following experiments to evaluate the CO_2 capture performances of the sample after all cycles and avoid the random error. The gas flow rates were controlled by mass flow meters to meet the designed reaction atmosphere and steam was generated from a steam generator. All gases were premixed evenly before they were sent into reactors together. The total flow rate was 2 L/min. The samples were calcined in the conditions of 850 °C—100% H_2O, 850 °C—85% H_2O/15% CO_2, or 920 °C—70% CO_2/N_2, and carbonated at 700 °C under 15% CO_2/N_2 or 10% H_2O/15% CO_2/N_2. The cyclic CO_2 capture capacities and the carbonation conversions of the samples were calculated from the recorded weight changes during repeated calcination and carbonation reactions, as shown in Equations (1) and (2).

$$C_N = \frac{m_N - m_{\mathrm{cal},N}}{m_0}, \tag{1}$$

$$X_N = \frac{m_N - m_{\mathrm{cal},N}}{m_0} \cdot \frac{M_{\mathrm{CaCO_3}}}{M_{\mathrm{CO_2}}}, \tag{2}$$

where N is the number of calcination/carbonation cycles; C_N and X_N denote the CO_2 capture capacity and the carbonation conversion of the sorbent after the Nth cycle, respectively; m_0 is the initial mass of the sorbent after calcination, g; m_N and $m_{\mathrm{cal},N}$ are the masses of the sorbent after the Nth carbonation and calcination, respectively, g; and M_{CaCO3} and M_{CO2} are the molar masses of $CaCO_3$ and CO_2, respectively, g/mol.

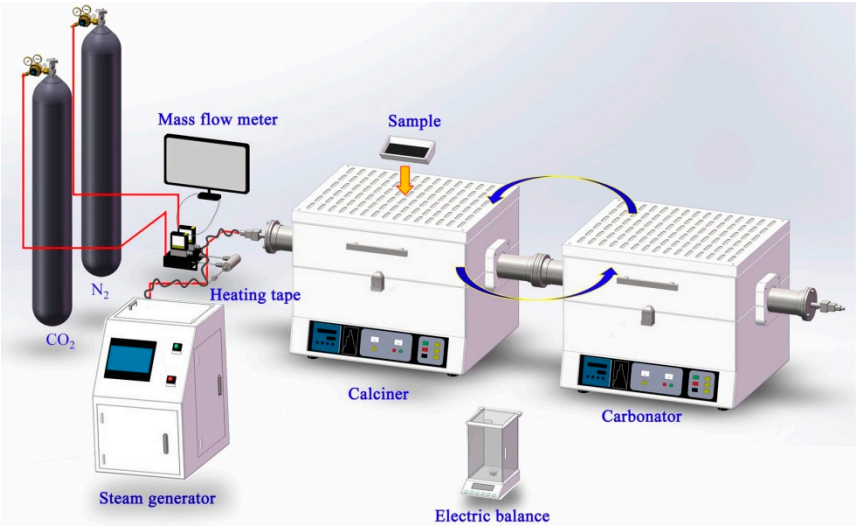

Figure 1. Diagram of dual fixed-bed reactor (DFBR) with steam generator.

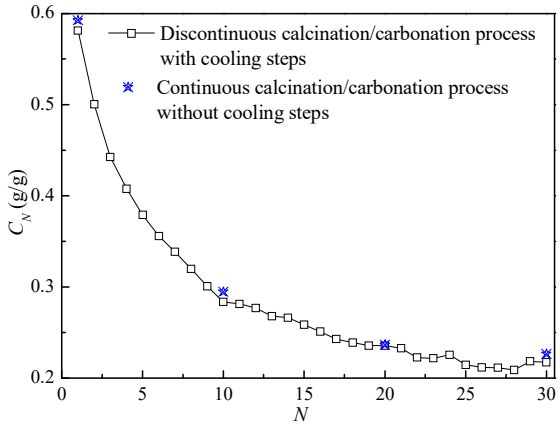

Figure 2. Preliminary experiments on calcination/carbonation processes with/without cooling steps (carbide slag as the sample, carbonation in 15% CO_2/N_2 at 700 °C for 20 min, calcination in 100% N_2 at 850 °C).

The CO_2 capture kinetics of the synthetic sorbent was evaluated by a thermo-gravimetric analyzer (TGA, Mettler Toledo TGA/SDTA851^e). Around 5 mg of the pristine sample or the sample that had experienced 10 cycles in DFBR was placed in an alumina pan and put in the furnace together. Temperature was raised from ambient temperature to the carbonation temperature of 700 °C at a rate of 30 °C/min under a N_2 flow of 120 mL/min. Once the temperature was reached, the N_2 flow was switched to a flow of 120 mL/min CO_2. Carbonation was performed for 30 min. The mass change of the sample was continuously monitored and the CO_2 capture capacity (C_N) and the CO_2 capture rate (μ_t) were calculated, respectively, as shown in Equations (1) and (3).

$$\mu_t = \frac{dC_N}{dt} \tag{3}$$

2.3. Characterization

Selected samples were characterized with regards to crystalline phase using X-ray diffraction instrument (XRD, D/Max-III, Rigaku Co., Ltd, Japan), pore characteristics using N_2 adsorption equipment (Micromeritics ASAP 2020-M, Micrometer Co., Ltd, Shanghai, China), and micro-morphologies using field emission scanning electron microscope (FE-SEM, SUPRATM 55, Zeiss Co., Ltd, Germany).

3. Results and Discussion

3.1. Composition of the Synthetic Sorbent

The XRD patterns of the synthetic sorbents are shown in Figure 3. It can be found that the phase compositions of the synthetic sorbent are unchanged when the CaO/Al_2O_3 ratios are different. The two synthetic sorbents are mainly composed of CaO and $Ca_{12}Al_{14}O_{33}$. The peak values of HT10 are higher than those of HT5, which indicates that the $Ca_{12}Al_{14}O_{33}$ content is higher with a lower CaO/Al_2O_3 ratio. Apparently, CaO is derived from the decomposition of the acetic acid-washed carbide slag, i.e., calcium acetate. In addition, Al_2O_3 is generated by the decomposition of aluminum nitrate. A portion of CaO reacts with Al_2O_3 at a high temperature during the preparation process and $Ca_{12}Al_{14}O_{33}$ is formed, as shown in Equation (4) [44,45]. The computed mass ratio of $CaO/Ca_{12}Al_{14}O_{33}$ in HT5 and HT10 is about 90:10 and 80:20, respectively. $Ca_{12}Al_{14}O_{33}$ is one of the effective support materials for CaO-based sorbents, because of its high stability and separation effect on CaO particles under a high temperature [32,46].

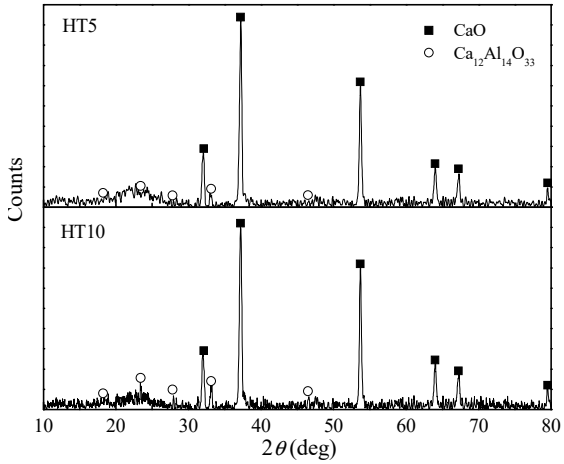

Figure 3. X-ray diffraction (XRD) pattern of synthetic sorbents HT5 and HT10.

$$12CaO + 7Al_2O_3 \rightarrow Ca_{12}Al_{14}O_{33} \quad (4)$$

3.2. Comparison of Preparation Methods

The cyclic CO_2 capture capacities of synthetic sorbents prepared by different methods are analyzed, as shown in Figure 4. The initial CO_2 capture capacities, C_1, of HT5 and WM5 are 0.63 g/g and 0.61 g/g, which are 8.9% and 4.3% higher, respectively, than that of carbide slag. This phenomenon is mainly because of the fact that $Ca(OH)_2$ in carbide slag reacts with acetic acid to form $Ca(CH_3COO)_2$. $Ca(CH_3COO)_2$ decomposes at a high temperature and thus gas is released, leaving a large number of pores in the synthetic sorbents. As a result, the diffusion resistance of CO_2 during carbonation process is weakened and the CO_2 capture performance of HT5 is improved. During the following 10 cycles, the CO_2 capture capacity of WM5 decreases by 13.2%, while the value for HT5 is only about 8%. Given that the combustion of carbon template contributes to the formation of a porous microstructure, the well-distributed CaO and $Ca_{12}Al_{14}O_{33}$ results in a stable and porous surface of the synthetic sorbent when the hydrothermal template method is applied. Therefore, HT5 shows a higher CO_2 capture capacity than WM5. In addition, C_1 of HT5 is 38% higher than the synthetic sorbent with the addition of 5% cement. After 10 cycles, C_{10} of HT5 is 1.5 times as high as that of the one with 5% cement. This indicates that the synthetic sorbent prepared using acetic acid-washed carbide slag and aluminum nitrate as soluble precursors possesses better CO_2 capture performance than that prepared using carbide slag and cement as insoluble precursors. However, from an economic point of view, the use of carbide slag and cement is more cost-effective than the use of acetic acid-washed carbide slag and aluminum nitrate in preparation. With the increase in cycle numbers, the CO_2 capture capacities of the three synthetic sorbents are relatively stable, and attenuations of the CO_2 capture capacities are slower than that of carbide slag. After the 10 cycles, C_{10} of HT5 is 0.58 g/g, which is 1.1 times and 2 times those of WM5 and carbide slag, respectively. To sum up, HT5 achieves the best CO_2 capture performance during the cyclic CO_2 capture process.

The comparisons between CO_2 capture capacities of HT5 and diverse CaO-based, calcium aluminates-stabilized sorbents reported elsewhere are summarized in Table 2. Li et al. [31] fabricated a $CaO/Ca_3Al_2O_6$ sorbent using the same calcium and aluminum precursors as this study by the combustion method. C_{10} of the synthetic sorbent is 0.45 g/g, which is about 20% lower than the value of HT5. Luo et al. [47] reported the synthesis of sorbents supported by different materials, such as Ca_2MnO_4, La_2O_3, $Ca_{12}Al_{14}O_{33}$, and MgO, using the sol-gel technique, and conformed better performance of the $CaO/Ca_{12}Al_{14}O_{33}$ sorbent than others. However, a large amount of calcium nitrate decomposes under the high-temperature preparation process and toxic nitrogen oxides, which are adverse to the environment and human health, are released with it. This is the disadvantage of this

method. Broda et al. [48] used carbon gel as a template to fabricate synthetic CaO-based sorbents containing $Ca_{12}Al_{14}O_{33}$, which achieved C_{10} of 0.56 g/g when the calcination atmosphere was 100% N_2. In comparison, it can be found that HT5 shows superior CO_2 capture performance. Therefore, the synthetic sorbent prepared by hydrothermal template method is a kind of sorbent with good CO_2 capture performance and cyclic stability.

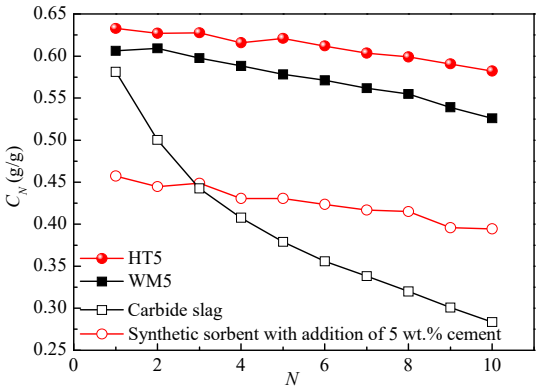

Figure 4. CO_2 capture capacities of sorbents prepared using different methods (glucose addition of 1 mol/L for the hydrothermal template method, pre-calcination at 600 °C for 1 h; carbonation in 15% CO_2/N_2 at 700 °C for 20 min, calcination in 100% N_2 at 850 °C for 10 min).

Table 2. Comparison of CO_2 capture performance for different CaO-based, calcium aluminates-stabilized sorbents.

Calcium Aluminates	CaO Ratios (wt.%)	Precursors	Methods	Reaction Conditions	C_{10}
$Ca_3Al_2O_6$ [41]	90	Carbide slag; $Al(NO_3)_3$	Combustion	Carbonation: T_1, A_1, t_3; Calcination: T_3, A_3, t_1	0.45
$Ca_9Al_6O_{18}$ [49]	90	$Ca(C_6H_5O_7)_2$; $Al(NO_3)_3$	Mixing	Carbonation: T_1, A_1, t_3; Calcination: 800 °C, A_3, t_1	0.55
$Ca_{12}Al_{14}O_{33}$ [47]	80	$Ca(NO_3)_2$; $Al(NO_3)_3$	Sol-gel	Carbonation: T_2, A_1, 2.5 min; Calcination: 950 °C, CO_2, 2.5 min	0.35
$Ca_{12}Al_{14}O_{33}$ [36]	75	Sol-gel CaO; Cement	Dry mixing	Carbonation: T_2, A_1, 15 min; Calcination: T_3, A_3, t_1	0.48
$Ca_{12}Al_{14}O_{33}$ [37]	90	Limestone; Cement	Wet mixing	Carbonation: T_2, A_1, t_3; Calcination: 900 °C, A_3, t_1	0.28
$Ca_{12}Al_{14}O_{33}$ [48]	90	$Ca(NO_3)_2$; $Al(NO_3)_3$	Carbon gel Templating	Carbonation:750 °C, 60%CO_2, t_2; Calcination: 750 °C, A_3, t_2	0.56
$Ca_{12}Al_{14}O_{33}$ (this work)	90	Carbide slag; $Al(NO_3)_3$	Hydrothermal Templating	Carbonation: T_1, A_1, t_2; Calcination: T_3, A_3, t_1	0.58

Note: T_1 denotes 650 °C; T_2 denotes 700 °C; T_3 denotes 850 °C; A_1 denotes 15% CO_2/N_2; A_2 denotes 20% CO_2/N_2; A_3 denotes 100% N_2; t_1 denotes 10 min; t_2 denotes 20 min; t_3 denotes 30 min.

3.3. *Effect of Support Ratios*

The influence of the Al_2O_3 ratio (2.5–10%) in the preparation process on the cyclic CO_2 capture performance of synthetic sorbents is studied, as shown in Figure 5. It can be seen from Figure 5a that all of synthetic sorbents prepared by the hydrothermal template method show more stable CO_2 capture performance than carbide slag under the calcination condition of 100% N_2. After 10 cycles, C_{10} of HT2.5, HT5, HT7.5, and HT10 is 0.62 g/g, 0.58 g/g, 0.57 g/g, and 0.52 g/g, respectively, which is only 4.7%, 8%, 5.5%, and 3% lower than C_1 of those sorbents. The results show that the sintering resistance of synthetic sorbents can be improved with the addition of Al_2O_3 in the range of 2.5–10%. This is because of $Ca_{12}Al_{14}O_{33}$ generated by the solid-phase reaction between Al_2O_3 and CaO, which effectively improves the anti-sintering performance of the synthetic sorbents and the cyclic stability of CO_2 capture. As the amount of Al_2O_3 increases, more CaO reacts with Al_2O_3 to generate $Ca_{12}Al_{14}O_{33}$,

resulting in the decrease of CaO content and the theoretical maximum CO_2 capture capacity of the synthetic sorbent. Therefore, there is an appropriate amount of Al_2O_3 to enable the synthetic sorbent to obtain higher CO_2 capture performance and cycling stability.

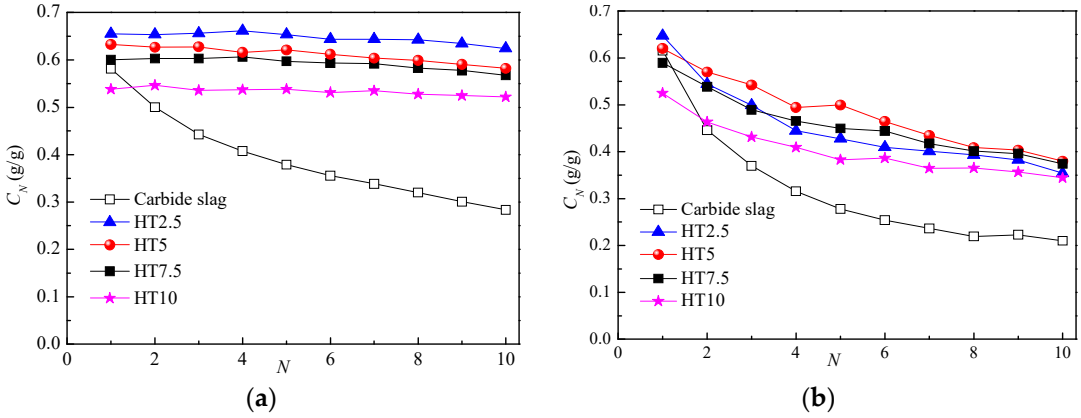

Figure 5. CO_2 capture capacities of synthetic sorbents prepared using hydrothermal template method under the (**a**) mild and (**b**) harsh calcination conditions (carbonation in 15% CO_2/N_2 at 700 °C for 20 min, calcination (mild) in 100% N_2 at 850 °C or (harsh) in 70% CO_2/N_2 at 920 °C for 10 min).

In the industrial application, the regeneration of CaO-based sorbents is carried out under a high concentration of CO_2, which corresponds to a high calcination temperature. Valverde et al. [50] and Manovic et al. [51] both came to the conclusion that CaO particles suffered from severe sintering under the calcination condition of 920 °C, 70% CO_2/N_2. Therefore, the high concentration of N_2 is a mild calcination condition and the high concentration of CO_2 is a relatively harsh calcination condition. As shown in Figure 5b, the CO_2 capture capacities of synthetic sorbents decrease slowly with the increase of cycle numbers under the harsh calcination condition, while that of carbide slag decreases rapidly. For example, the calculated attenuation ratios of HT2.5, HT5, HT7.5, and HT10 are 45.3%, 38.8%, 36.6%, and 34.4%, respectively, during the following 10 cycles, while the value of carbide slag is as high as 65.9%. This suggests that the synthetic sorbents show relatively higher sintering resistance than carbide slag. After 10 cycles, C_{10} of HT2.5, HT5, HT7.5, and HT10 is 68.6%, 80.9%, 78.2%, and 64.1% higher, respectively, than that of carbide slag. Although C_1 of HT2.5 is higher than that of HT5, its CO_2 capture capacity decreases more noticeably with the number of cycles. At the 10th cycle, HT5 is the best performing synthetic sorbent in this set of experiments, with a CO_2 capture capacity of 0.38 g/g. The average CO_2 capture capacity of HT5 is 0.48 g/g in the following 10 cycles, which is 7% higher than that of HT2.5. By comprehensive consideration of CO_2 capture capacity and stability, the following experiments are focused on HT5.

3.4. Effect of Reaction Conditions

Studies have shown that O_2/H_2O combustion is a promising technology with many advantages, such as easy operation and energy saving, compared with O_2/CO_2 combustion. Therefore, the calcination atmosphere with a high concentration of steam and a high concentration of CO_2 belong to actual calcination conditions. The cyclic CO_2 capture capacities of HT5 under three calcination conditions (850 °C—100% H_2O, 850 °C—85% H_2O/15% CO_2, and 920 °C—70% CO_2/N_2) are evaluated, as shown in Figure 6. Both HT5 and carbide slag show the best CO_2 capture performance under the calcination atmosphere of 100% H_2O. C_{10} of HT5 and carbide slag is 0.46 g/g and 0.28 g/g, which is 21.9% and 34.6% higher, respectively, than those calcined under the high concentration of CO_2. Moreover, C_{10} of carbide slag under the calcination atmosphere of 85% H_2O/15% CO_2 is 10.6% higher than that when the calcination under the high concentration of CO_2 is applied, although this difference between C_{10} of HT5 under the two conditions is not significant. Studies have shown that the presence of CO_2 in the calcination atmosphere accelerates the process of sintering and reduces the specific surface

area of CaO-based sorbents [52,53]. The undiminished CO_2 capture capacity of HT5 under the high concentration of CO_2 means that HT5 has better sintering resistance than carbide slag. Calcination under the high concentration of H_2O is more conducive to the cyclic stability of HT5 during the CO_2 capture process. HT5 shows better CO_2 capture performance than carbide slag under all of three calcination conditions. The average CO_2 capture capacities of HT5 in the 10 cycles are 1.4 times, 1.4 times, and 1.5 times as high as those of carbide slag, respectively.

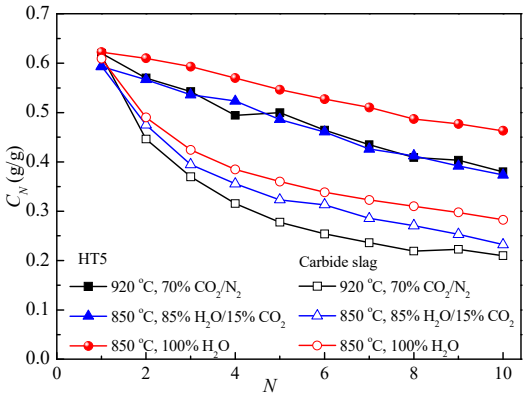

Figure 6. Effects of calcination conditions on the CO_2 capture capacities of HT5 (carbonation in 15% CO_2/N_2 at 700 °C for 20 min, calcination for 10 min).

The effect of H_2O existing in the carbonation atmosphere on the CO_2 capture by HT5 is studied under the harsh calcination condition, as shown in Figure 7. It is apparent that HT5 and carbide slag achieve higher CO_2 capture capacities in different degrees with the presence of 10% H_2O in the carbonation atmosphere. C_{10} of HT5 and carbide slag is increased by 9.2% and 56.2%, respectively, in the presence of H_2O. The result shows that, by contrast, the presence of H_2O has a greater effect on promoting the CO_2 capture performance of carbide slag. This is because the presence of H_2O enhances the proliferation of O^{2-} ions in CaO [54,55]. Carbide slag suffers from serious sintering in the cyclic process, which leads to less porous structure. On this occasion, O^{2-} ions must penetrate the $CaCO_3$ product layer in carbide slag to contact with external CO_2. Therefore, the CO_2 diffusion resistance for carbide slag increases. The good sintering resistance of HT5 is conducive to the relative stability of pore structure, which results in a lower diffusion resistance of CO_2. This is the explanation for the more pronounced influence of H_2O on the CO_2 capture performance of carbide slag than that of HT5. After 10 cycles, C_{10} of HT5 carbonated with the presence of H_2O exceeds that of carbide slag by 26.5%.

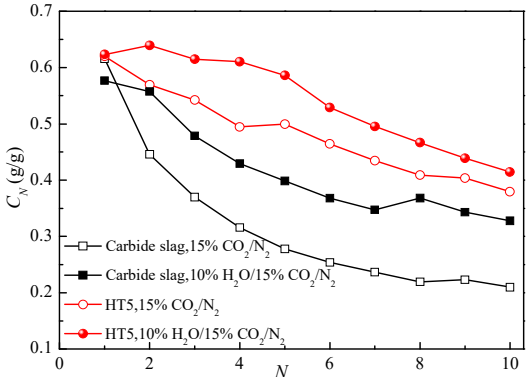

Figure 7. Effects of H_2O existing in the carbonation atmosphere on the CO_2 capture capacities of HT5 (carbonation at 700 °C for 20 min, calcination in 70% CO_2/N_2 at 920 °C for 10 min).

3.5. CO_2 Capture during Extended Cycles

Figure 8 shows the CO_2 capture performance of HT5 during 100 cycles under mild and harsh calcination conditions. It is interesting to notice that the capture performance degradation mainly occurs in the previous 30 cycles. After 100 cycles, the CO_2 capture capacities of HT5 under mild and harsh calcination conditions decrease by 51.2% and 61.1%, respectively, while those of carbide slag decrease by 69.7% and 78%, respectively. Therefore, HT5 possesses better stability during the long-term cycles. Under the harsh calcination condition, the average CO_2 capture capacity of HT5 in the 100 cycles is 0.29 g/g, which is 72.1% higher than the value of carbide slag. C_{100} of HT5 is 0.31 g/g and 0.24 g/g under the mild and harsh calcination conditions, respectively, which are both 1.8 times as high as those of carbide slag under the same conditions. In conclusion, HT5 has better long-term CO_2 capture performance under both mild and harsh calcination conditions. To maintain the overall CO_2 capture efficiency at a high level in the industrial application, deactivated sorbents are continually discharged and a great quantity of fresh sorbents are added during the CaL process [8]. Studies have shown that energy consumption apparently decreases with the increased cyclic CO_2 capture capacity of the calcium-based sorbents [56,57]. Therefore, the utilization of HT5 is supposed to result in the decrease in make-up sorbents and energy saving compared with the situation when carbide slag is applied.

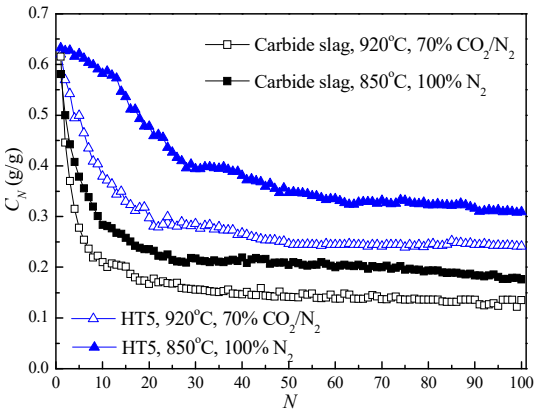

Figure 8. Long-term CO_2 capture capacities of HT5 (carbonation in 15% CO_2/N_2 at 700 °C for 20 min, calcination for 10 min).

3.6. Apparent CO_2 Capture Kinetics

Figure 9a,b show the CO_2 capture capacities and the apparent CO_2 capture rates of HT5 with time during the 1st and 11th carbonation processes, respectively. The CO_2 capture capacities of HT5 and carbide slag increase rapidly with time in the previous 50 s and the increase becomes slower after 50 s, as shown in Figure 9a. In the 1st carbonation, the CO_2 capture capacity of HT5 is almost same as that of carbide slag within 100 s, gradually higher than that of carbide slag after 100 s, and eventually 4.3% higher than that of carbide slag after 30 min. In the 11th carbonation, The CO_2 capture capacities of HT5 and carbide slag are at lower levels compared with those in the 1st carbonation as a result of high-temperature sintering. The difference is a significant reduction in the CO_2 capture capacity of carbide slag in the previous 100 s. The final CO_2 capture capacity of HT5 is obviously higher and the cycle stability is better than that of carbide slag.

The apparent CO_2 capture rates of HT5 and carbide slag are shown in Figure 9b. During the 1st and 11th carbonation processes, HT5 and carbide slag have relatively high CO_2 capture rates in the previous 75 s, and the CO_2 capture rates decreases gradually after 75 s. In the 1st carbonation, the CO_2 capture rates of HT5 and carbide slag reach their maximum values at around 45 s. The CO_2 capture rate of carbide slag is slightly higher than that of HT5 in the previous 45 s, while it falls rapidly and remains lower than that of HT5 after 45 s. This phenomenon suggests that the more CO_2 diffusion degree in

HT5 contributes to the process of carbonation. The CO_2 capture rates of HT5 and carbide slag in the 11th carbonation are relatively lower than those in the 1st carbonation. However, the increased cycle number has less impact on carbonation performance of HT5 than that of carbide slag. The maximum CO_2 capture rate of carbide slag moves forward to 35 s and the duration of chemical reaction-controlled stage is shortened. After 10 cycles, HT5 possesses higher CO_2 capture rate than carbide slag.

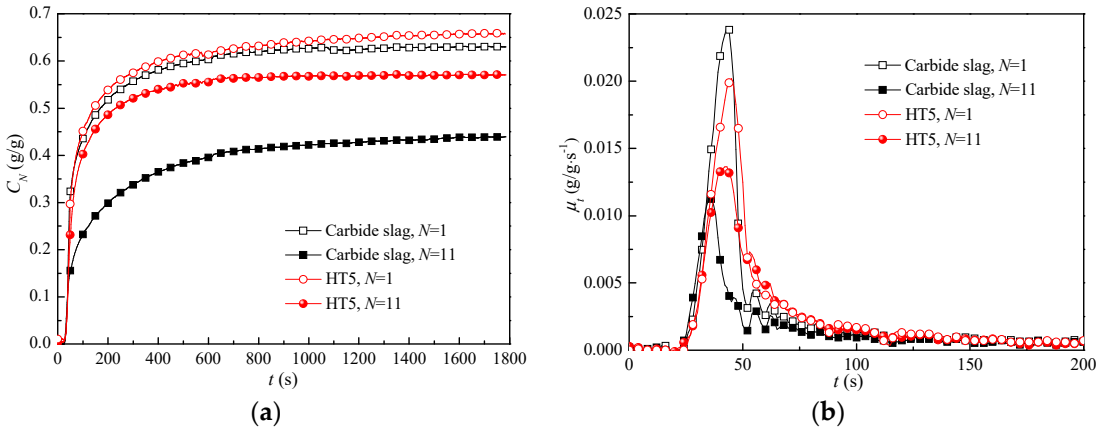

Figure 9. Apparent CO_2 capture kinetics of HT5 tested on thermo-gravimetric analyzer (TGA): (**a**) CO_2 capture capacities and (**b**) apparent CO_2 capture rates (carbonation in 15% CO_2/N_2 at 700 °C for 20 min, calcination in 100% N_2 at 850 °C).

The shrinking core model is used to describe the CO_2 capture kinetics because of its high accuracy [58,59]. At the chemical reaction-controlled and diffusion-controlled stages, the carbonation conversions of CaO-based sorbents with time are described as Equations (5) and (6) [60,61].

$$1-(1-X_N)^{1/3} = k_C(P_{CO_2}-P_{eq})t, \quad (5)$$

$$1-3(1-X_N)^{2/3}+2(1-X_N) = k_D(P_{CO_2}-P_{eq})t, \quad (6)$$

where k_C and k_D represent the apparent reaction rate constants at the two stages, respectively, $MPa^{-1}\cdot s^{-1}$. P_{eq} and P_{CO2} represent the equilibrium concentration and partial pressure of CO_2, respectively, MPa. By means of the linear fitting, the relations between carbonation conversion and time for HT5 and carbide slag at the two stages are obtained, as shown in Figure 10a,b. The value of k_C and k_D are calculated accordingly and the results are given in Table 3. According to the correlation coefficients, that is, R^2, the conclusion can be drawn that the shrinking core model matches better with the results at the chemical reaction-controlled stage than those at the diffusion-controlled stage. The apparent reaction rate constants of HT5 and carbide slag are reduced with cycles. k_C is much higher than k_D, which suggests that the CO_2 capture rate of the CaO-based sorbent at the chemical reaction-controlled stage is far above that at the diffusion-controlled stage. In the 1st carbonation, k_C of carbide slag is higher than that of HT5, while k_D of carbide slag is relatively lower. This phenomenon indicates that the structure of HT5 is more favorable to the diffusion of CO_2 inside the sorbents, and thus the process of carbonation reaction. After 10 cycles, k_C and k_D of HT5 are 26.3% and 58.9% higher than those of carbide slag, respectively. Therefore, the superiority of the synthetic sorbent prepared using the hydrothermal template method on the CO_2 capture kinetics mainly reflects at the diffusion-controlled stage.

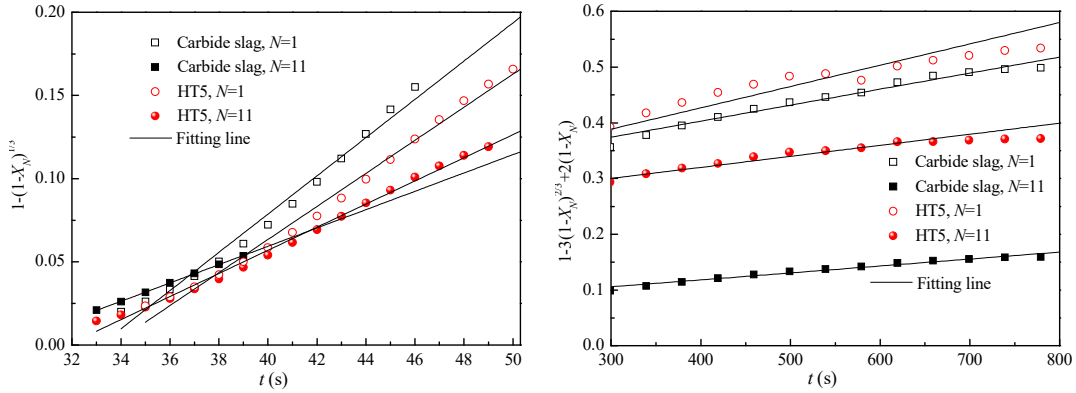

Figure 10. Carbonation kinetics curves of HT5 at (**a**) the chemical reaction-controlled stage and (**b**) the diffusion-controlled stage fitted by the shrinking core model (carbonation in 15% CO_2/N_2 at 700 °C for 20 min, calcination in 100% N_2 at 850 °C).

Table 3. Apparent reaction rate constants of HT5 and carbide slag after fitting.

Samples.	*N*	k_C	R^2	$k_D \times 10^3$	R^2
Carbide slag	1	0.119	0.983	2.978	0.968
HT5	1	0.103	0.990	3.964	0.942
Carbide slag	11	0.057	1	1.292	0.974
HT5	11	0.072	0.994	2.054	0.959

3.7. Microstructure Analysis

The apparent morphologies of HT5 and carbide slag after 10 cycles are observed by SEM apparatus, as shown in Figure 10. Carbide slag has smooth and dense surface morphology, as shown in Figure 11a. This phenomenon is attributed to sintering. Low porosity hinders CO_2 diffusion, which results in poor CO_2 capture performance of carbide slag under the harsh calcination condition. It can be seen from Figure 11b that HT5 undergoing 10 cycles under the harsh calcination condition is sphere-shaped. With a magnification factor of 50,000, it can be found that the average grain size of HT5 is smaller than that of carbide slag, as illustrated in Figure 11c,d. In addition, HT5 has larger porosity than carbide slag. The result proves the superiority of the pore structure of HT5 again, and this is the reason for the high CO_2 capture capacity of HT5 under harsh calcination conditions.

N_2 adsorption analysis is conducted on the pore characteristics of HT5 and carbide slag after 10 cycles calcined under the harsh calcination condition, as shown in Figure 12. The N_2 adsorption–desorption isotherms, Figure 12a, reveal the type IV curves and the presence of a hysteresis loop for both HT5 and carbide slag. Thus, they have mesoporous structures and the maximum quantity adsorbed of the synthetic sorbent is higher than that of carbide slag. In order to further explore the mechanism of the influence of the pore properties on the CO_2 capture characteristics of the synthetic sorbent, the surface areas and pore volumes of HT5 and carbide slag are analyzed, as shown in Table 4. After 10 cycles, the surface area and the pore volume of HT5 are 7 m^2/g and 0.038 cm^3/g, respectively, which are more than double those of calcined carbide slag. Figure 12b shows the pore volume distribution of HT5. It can be clearly seen that the pore volume of the synthetic sorbent in the range of 2–100 nm is significantly improved after the preparation process by the hydrothermal template method. Studies have shown that the CO_2 capture rate that CaO-based sorbents can achieve is mainly determined by the pores within the range of 10–100 nm [62]. The cumulative pore volume of calcined carbide slag within the range of 10–100 nm is 0.0009 cm^3/g, while the cumulative pore volume of HT5 within the same range is 0.0022 cm^3/g, 2.4 times as high as that of calcined carbide slag. The pore structure of HT5 is more conducive than that of carbide slag to the diffusion of CO_2 and the carbonation reaction of inner CaO. This result is consistent with the above calculated reaction

kinetics, which indicates that the good pore structure of HT5 is the main reason for the high reaction rate constant.

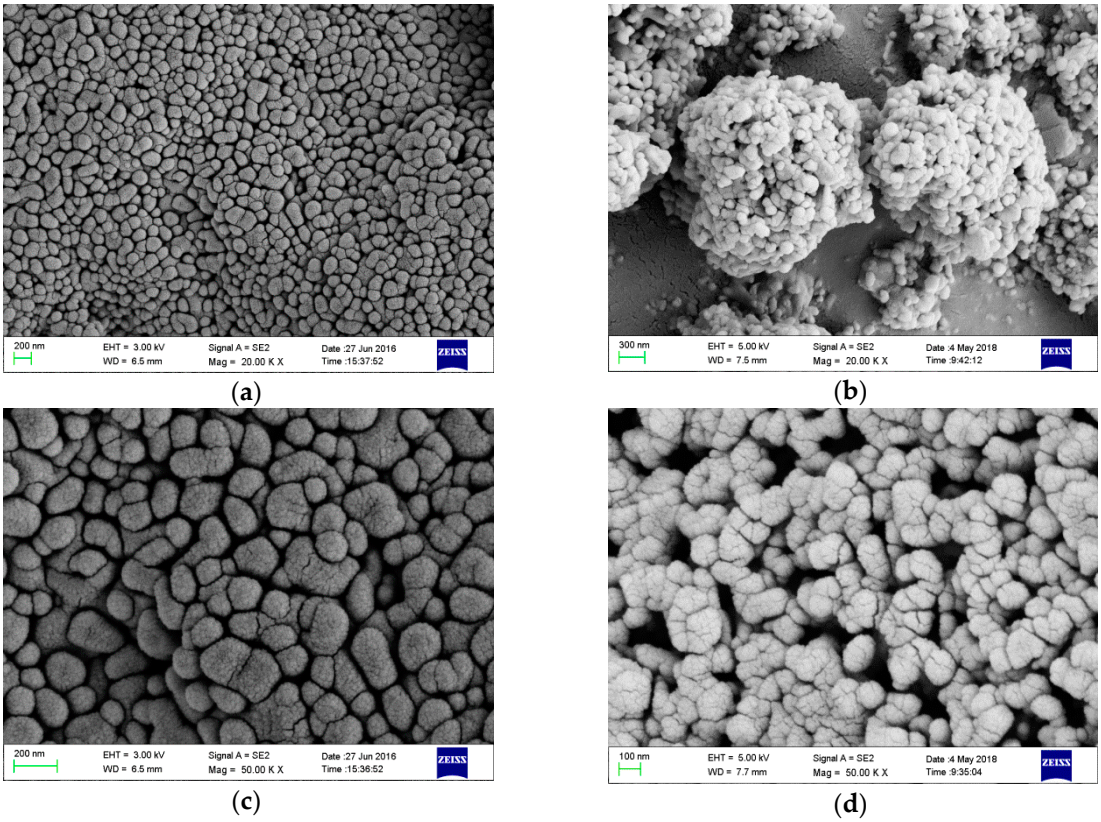

Figure 11. Scanning electron microscope (SEM) images of (**a**), (**c**) carbide slag and (**b**), (**d**) HT5 after 10 cycles with different magnification factors, ×20,000 and ×50,000 (carbonation in 15% CO_2/N_2 at 700 °C for 20 min, calcination in 70% CO_2/N_2 at 920 °C for 10 min).

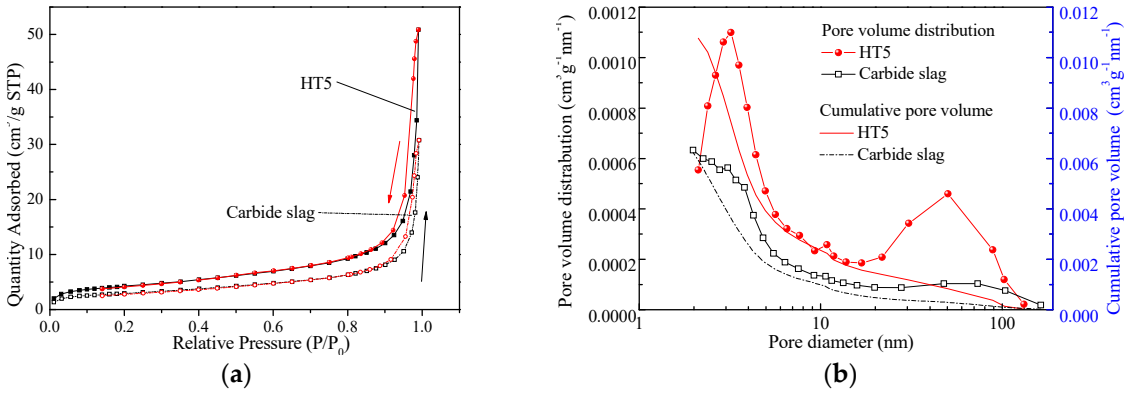

Figure 12. Pore characteristics of HT5 and carbide slag: (**a**) N_2 adsorption–desorption isotherms, (**b**) pore volume distributions after 10 cycles (carbonation in 15% CO_2/N_2 at 700 °C for 20 min, calcination in 70% CO_2/N_2 at 920 °C for 10 min).

Table 4. Surface areas and pore volumes of HT5 and carbide slag (carbonation in 15% CO_2/N_2 at 700 °C for 20 min, calcination in 70% CO_2/N_2 at 920 °C for 10 min).

Samples	*N*	BET Surface Area m^2/g	BJH Pore Volume cm^3/g
Carbide slag	0	10	0.048
	10	3	0.017
HT5	0	12	0.053
	10	7	0.038

Note: BET denotes Brunner–Emmet–Teller; BJH denotes Barrett-Joyner-Halenda.

4. Conclusions

In this work, a carbide slag-based, $Ca_{12}Al_{14}O_{33}$-stabilized sorbent was prepared by the hydrothermal template method with soluble calcium and aluminum sources. The main conclusions are as follows. The synthetic sorbent prepared using acetic acid-washed carbide slag and aluminum nitrate as soluble precursors has higher initial CO_2 capture capacity than that prepared using carbide slag and cement as insoluble precursors. When the addition amount of Al_2O_3 is 5%, the CO_2 capture capacities of the synthetic sorbent after 30 cycles decrease by 37.7% and 53.9% under mild and harsh calcination conditions, respectively, while those of carbide slag decrease by 62.6% and 74.7%, respectively. The synthetic sorbent possesses higher CO_2 capture performance and sintering resistance. The calcination condition of high concentration of steam is more favorable for the synthetic sorbent to maintain the cyclic stability in the CO_2 capture process. After 10 cycles, the calculated reaction rate constants of the synthetic sorbent are 26.3% and 58.9% higher, respectively, than those of carbide slag. Specifically, the good pore structure is the main reason for the high CO_2 capture capacity of the synthetic sorbent.

Author Contributions: Conceptualization, X.M.; methodology, X.M.; project administration—Y.L.; validation, Y.Q. and Z.W.; writing—original draft preparation, X.M.; writing—review and editing, Y.L.

Acknowledgments: Financial support from National Natural Science Foundation of China (51876105) and the Fundamental Research Funds of Shandong University, China (2018JC039) is gratefully appreciated.

Conflicts of Interest: The authors declare no conflict of interest.

References

1. Nazir, S.; Bolland, O.; Amini, S. Analysis of combined cycle power plants with chemical looping reforming of natural gas and pre-combustion CO_2 capture. *Energies* **2018**, *11*, 147. [CrossRef]
2. Zaimes, G.G.; Beck, A.W.; Janupala, R.R.; Resasco, D.E.; Crossley, S.P.; Lobban, L.L.; Khanna, V. Multistage torrefaction and in situ catalytic upgrading to hydrocarbon biofuels: Analysis of life cycle energy use and greenhouse gas emissions. *Energy Environ. Sci.* **2017**, *10*, 1034–1050. [CrossRef]
3. Liu, F.; Zhao, F.; Liu, Z.; Hao, H. China's electric vehicle deployment: Energy and greenhouse gas emission impacts. *Energies* **2018**, *11*, 3353. [CrossRef]
4. Special Report on Global Warming of 1.5 °C. Available online: https://www.ipcc.ch/sr15/ (accessed on 23 May 2019).
5. Vanga, G.; Gattia, D.M.; Stendardo, S.; Scaccia, S. Novel synthesis of combined CaO-$Ca_{12}Al_{14}O_{33}$-Ni sorbent-catalyst material for sorption enhanced steam reforming processes. *Ceram. Int.* **2019**, *45*, 7594–7605. [CrossRef]
6. Fernández, J.; Sotenko, M.; Derevschikov, V.; Lysikov, A.; Rebrov, E.V. A radiofrequency heated reactor system for post-combustion carbon capture. *Chem. Eng. Process. Process Intensif.* **2016**, *108*, 17–26. [CrossRef]
7. Sotenko, M.; Fernández, J.; Hu, G.; Derevschikov, V.; Lysikov, A.; Parkhomchuk, E.; Rebrov, E.V. Performance of novel CaO-based sorbents in high temperature CO_2 capture under RF heating. *Chem. Eng. Process.* **2017**, *122*, 487–492. [CrossRef]
8. Su, C.; Duan, L.; Donat, F.; Anthony, E.J. From waste to high value utilization of spent bleaching clay in synthesizing high-performance calcium-based sorbent for CO_2 capture. *Appl. Energy* **2018**, *210*, 117–126. [CrossRef]

9. Sisinni, M.; Di Carlo, A.; Bocci, E.; Micangeli, A.; Naso, V. Hydrogen-rich gas production by sorption enhanced steam reforming of woodgas containing tar over a commercial Ni catalyst and calcined dolomite as CO_2 sorbent. *Energies* **2013**, *6*, 3167–3181. [CrossRef]
10. Fan, Z.; Chen, L.; Liu, F.; Liu, K. Analytical evaluation of CaO-CO_2 loop for CO_2 removal. *CIESC J.* **2015**, *66*, 3233–3241.
11. Dou, B.; Wang, C.; Song, Y.; Chen, H.; Jiang, B.; Yang, M.; Xu, Y. Solid sorbents for In-Situ CO_2 removal during sorption-enhanced steam reforming process: A review. *Renew. Sustain. Energy Rev.* **2016**, *53*, 536–546. [CrossRef]
12. Bhatta, L.K.G.; Subramanyam, S.; Chengala, M.D.; Olivera, S.; Venkatesh, K. Progress in hydrotalcite like compounds and metal-based oxides for CO_2 capture: A review. *J. Clean. Prod.* **2015**, *103*, 171–196. [CrossRef]
13. Blamey, J.; Zhao, M.; Manovic, V.; Anthony, E.J.; Dugwell, D.R.; Fennell, P.S. A shrinking core model for steam hydration of CaO-based sorbents cycled for CO_2 capture. *Chem. Eng. J.* **2016**, *291*, 298–305. [CrossRef]
14. Salaudeen, S.A.; Acharya, B.; Dutta, A. CaO-based CO_2 sorbents: A review on screening, enhancement, cyclic stability, regeneration and kinetics modelling. *J. CO_2 Util.* **2018**, *23*, 179–199. [CrossRef]
15. Valverde, J.M.; Sanchez-Jimenez, P.E.; Perejon, A.; Perez-Maqueda, L.A. Role of looping-calcination conditions on self-reactivation of thermally pretreated CO_2 sorbents based on CaO. *Energy Fuels* **2013**, *27*, 3373–3384. [CrossRef]
16. Chen, Z.; Song, H.S.; Portillo, M.; Lim, C.J.; Grace, J.R.; Anthony, E.J. Long-term calcination/carbonation cycling and thermal pretreatment for CO_2 capture by limestone and dolomite. *Energy Fuels* **2009**, *23*, 1437–1444. [CrossRef]
17. Zhao, P.; Sun, J.; Li, Y.; Wang, K.; Yin, Z.; Zhou, Z.; Su, Z. Synthesis of efficient CaO sorbents for CO_2 capture using a simple organometallic calcium-based carbon template route. *Energy Fuels* **2016**, *30*, 7543–7550. [CrossRef]
18. Ping, H.; Wu, S. CO_2 sorption durability of Zr-modified nano-CaO sorbents with cage-like hollow sphere structure. *ACS Sustain. Chem. Eng.* **2016**, *4*, 2047–2055. [CrossRef]
19. Hu, Y.; Liu, W.; Jian, S.; Li, M.; Yang, X.; Yang, Z.; Liu, X.; Xu, M. Structurally improved CaO-based sorbent by organic acids for high temperature CO_2 capture. *Fuel* **2016**, *167*, 17–24. [CrossRef]
20. Zhang, Z.; Pi, S.; He, D.; Qin, C.; Ran, J. Investigation of pore-formers to modify extrusion-spheronized CaO-based pellets for CO_2 capture. *Processes* **2019**, *7*, 62. [CrossRef]
21. Sun, J.; Liu, W.; Chen, H.; Zhang, Y.; Hu, Y.; Wang, W.; Li, X.; Xu, M. Stabilized CO_2 capture performance of extruded-spheronized CaO-based pellets by microalgae templating. *Proc. Combust. Inst.* **2017**, *36*, 3977–3984. [CrossRef]
22. Zhang, Y.; Gong, X.; Chen, X.; Yin, L.; Zhang, J.; Liu, W. Performance of synthetic CaO-based sorbent pellets for CO_2 capture and kinetic analysis. *Fuel* **2018**, *232*, 205–214. [CrossRef]
23. Shi, J.; Li, Y.; Zhang, Q.; Ma, X.; Duan, L.; Zhou, X. CO_2 capture performance of a novel synthetic CaO/sepiolite sorbent at calcium looping conditions. *Appl. Energy* **2017**, *203*, 412–421. [CrossRef]
24. Rui, H.; Gao, J.; Wei, S.; Su, Y.; Qin, Y. Development of highly effective CaO@Al_2O_3 with hierarchical architecture CO_2 sorbents via a scalable limited-space chemical vapor deposition technique. *J. Mater. Chem. A* **2018**, *6*, 3462–3470.
25. Chen, H.; Wang, F.; Zhao, C.; Khalili, N. The effect of fly ash on reactivity of calcium based sorbents for CO_2 capture. *Chem. Eng. J.* **2017**, *309*, 725–737. [CrossRef]
26. Derevschikov, V.; Semeykina, V.; Bitar, J.; Parkhomchuk, E.; Okunev, A. Template technique for synthesis of CaO-based sorbents with designed macroporous structure. *Micropor. Mesopor. Mater.* **2017**, *238*, 56–61. [CrossRef]
27. Zhang, M.; Peng, Y.; Sun, Y.; Li, P.; Yu, J. Preparation of CaO-Al_2O_3 sorbent and CO_2 capture performance at high temperature. *Fuel* **2013**, *111*, 636–642. [CrossRef]
28. Wu, G.; Zhang, C.; Li, S.; Huang, Z.; Yan, S.; Wang, S.; Ma, X.; Gong, J. Sorption enhanced steam reforming of ethanol on Ni-CaO-Al_2O_3 multifunctional catalysts derived from hydrotalcite-like compounds. *Energy Environ. Sci.* **2012**, *5*, 8942–8949. [CrossRef]
29. Luo, C.; Zheng, Y.; Ding, N.; Wu, Q.L.; Zheng, C.G. SGCS-made ultrafine CaO/Al_2O_3 sorbent for cyclic CO_2 capture. *Chin. Chem. Lett.* **2011**, *22*, 615–618. [CrossRef]
30. Zhou, Z.; Xu, P.; Xie, M.; Cheng, Z.; Yuan, W. Modeling of the carbonation kinetics of a synthetic CaO-based sorbent. *Chem. Eng. Sci.* **2013**, *95*, 283–290. [CrossRef]

31. Li, Y.; Su, M.; Xie, X.; Wu, S.; Liu, C. CO_2 capture performance of synthetic sorbent prepared from carbide slag and aluminum nitrate hydrate by combustion synthesis. *Appl. Energy* **2015**, *145*, 60–68. [CrossRef]
32. Liu, W.; Feng, B.; Wu, Y.; Wang, G.; Barry, J.; Diniz da Costa, J.O.C. Synthesis of sintering-resistant sorbents for CO_2 capture. *Environ. Sci. Technol.* **2010**, *44*, 3093–3097. [CrossRef] [PubMed]
33. Chen, H.; Zhao, C.; Yu, W. Calcium-based sorbent doped with attapulgite for CO_2 capture. *Appl. Energy* **2013**, *112*, 67–74. [CrossRef]
34. Ridha, F.N.; Manovic, V.; Macchi, A.; Anthony, E.J. High-temperature CO_2 capture cycles for CaO-based pellets with kaolin-based binders. *Int. J. Greenh. Gas Control* **2012**, *6*, 164–170. [CrossRef]
35. Ridha, F.N.; Manovic, V.; Macchi, A.; Anthony, E.J. The effect of SO_2 on CO_2 capture by CaO-based pellets prepared with a kaolin derived $Al(OH)_3$ binder. *Appl. Energy* **2012**, *92*, 415–420. [CrossRef]
36. Luo, C.; Zheng, Y.; Xu, Y.; Ding, H.; Zheng, C.; Qin, C.; Feng, B. Cyclic CO_2 capture characteristics of a pellet derived from sol-gel CaO powder with $Ca_{12}Al_{14}O_{33}$ support. *Korean J. Chem. Eng.* **2015**, *32*, 934–938. [CrossRef]
37. Sun, J.; Liu, W.; Hu, Y.; Li, M.; Yang, X.; Zhang, Y.; Xu, M. Structurally improved, core-in-shell, CaO-based sorbent pellets for CO_2 capture. *Energy Fuels* **2015**, *29*, 6636–6644. [CrossRef]
38. Wu, Y.; Manovic, V.; He, I.; Anthony, E.J. Modified lime-based pellet sorbents for high-temperature CO_2 capture: Reactivity and attrition behavior. *Fuel* **2012**, *96*, 454–461. [CrossRef]
39. Li, Y.; Sun, R.; Liu, C.; Liu, H.; Lu, C. CO_2 capture by carbide slag from chlor-alkali plant in calcination/carbonation cycles. *Int. J. Greenh. Gas Control* **2012**, *9*, 117–123. [CrossRef]
40. Sun, J.; Liu, W.; Hu, Y.; Wu, J.; Li, M.; Yang, X. Enhanced performance of extruded-spheronized carbide slag pellets for high temperature CO_2 capture. *Chem. Eng. J.* **2016**, *285*, 293–303. [CrossRef]
41. Cheng, J.; Zhou, J.H.; Liu, J.Z.; Cao, X.Y.; Cen, K.F. Physicochemical characterizations and desulfurization properties in coal combustion of three calcium and sodium industrial wastes. *Energy Fuels* **2009**, *23*, 2506–2516. [CrossRef]
42. Li, Y.; Zhao, C.; Chen, H.; Liang, C.; Duan, L.; Zhou, W. Modified CaO-based sorbent looping cycle for CO_2 mitigation. *Fuel* **2009**, *88*, 697–704. [CrossRef]
43. Ma, X.; Li, Y.; Duan, L.; Anthony, E.; Liu, H. CO_2 capture performance of calcium-based synthetic sorbent with hollow core-shell structure under calcium looping conditions. *Appl. Energy* **2018**, *225*, 402–412. [CrossRef]
44. Martavaltzi, C.S.; Lemonidou, A.A. Parametric study of the CaO-$Ca_{12}Al_{14}O_{33}$ synthesis with respect to high CO_2 sorption capacity and stability on multicycle operation. *Ind. Eng. Chem. Res.* **2008**, *47*, 9537–9543. [CrossRef]
45. Martavaltzi, C.S.; Pampaka, E.P.; Korkakaki, E.S.; Lemonidou, A.A. Hydrogen production via steam reforming of methane with simultaneous CO_2 capture over CaO-$Ca_{12}Al_{14}O_{33}$. *Energy Fuels* **2010**, *24*, 2589–2595. [CrossRef]
46. Duan, L.; Yu, Z.; Erans, M.; Li, Y.; Manovic, V.; Anthony, E.J. Attrition study of cement-supported biomass-activated calcium sorbents for CO_2 capture. *Ind. Eng. Chem. Res.* **2016**, *55*, 9476–9484. [CrossRef]
47. Luo, C.; Zheng, Y.; Yin, J.J.; Qin, C.L.; Ding, N.; Zheng, C.G.; Feng, B. Effect of support material on carbonation and sulfation of synthetic CaO-based sorbents in calcium looping cycle. *Energy Fuels* **2013**, *27*, 4824–4831. [CrossRef]
48. Broda, M.; Muller, C.R. Synthesis of highly efficient, Ca-based, Al_2O_3-stabilized, carbon gel-templated CO_2 sorbents. *Adv. Mater.* **2012**, *24*, 3059–3064. [CrossRef]
49. Zhou, Z.; Qi, Y.; Xie, M.; Cheng, Z.; Yuan, W. Synthesis of CaO-based sorbents through incorporation of alumina/aluminate and their CO_2 capture performance. *Chem. Eng. Sci.* **2012**, *74*, 172–180. [CrossRef]
50. Valverde, J.M.; Medina, S. Crystallographic transformation of limestone during calcination under CO_2. *Phys. Chem. Chem. Phys.* **2015**, *17*, 21912–21926. [CrossRef]
51. Manovic, V.; Charland, J.P.; Blamey, J.; Fennell, P.S.; Lu, D.; Anthony, E.J. Influence of calcination conditions on carrying capacity of CaO-based sorbent in CO_2 looping cycles. *Fuel* **2009**, *88*, 1893–1900. [CrossRef]
52. Adánez, J.; de Diego, L.F.; García-Labiano, F. Calcination of calcium acetate and calcium magnesium acetate: Effect of the reacting atmosphere. *Fuel* **1999**, *78*, 583–592. [CrossRef]
53. Mai, M.C.; Edgar, T.F. Surface area evolution of calcium hydroxide during calcination and sintering. *AIChE J.* **2010**, *35*, 30–36. [CrossRef]
54. Labotka, T.C.; Cole, D.R.; Fayek, M.J.; Chacko, T. An experimental study of the diffusion of C and O in calcite in mixed CO_2-H_2O fluid. *Am. Miner.* **2011**, *96*, 1262–1269. [CrossRef]

55. Kronenberg, A.K.; Yund, R.A.; Giletti, B.J. Carbon and oxygen diffusion in calcite—Effects of Mn content and Ph_2O. *Phys. Chem. Miner.* **1984**, *11*, 101–112. [CrossRef]
56. Li, Y.; Zhao, C.; Chen, H.; Ren, Q.; Duan, L. CO_2 capture efficiency and energy requirement analysis of power plant using modified calcium-based sorbent looping cycle. *Energy* **2011**, *36*, 1590–1598. [CrossRef]
57. Zhang, W.; Li, Y.; He, Z.; Ma, X.; Song, H. CO_2 capture by carbide slag calcined under high-concentration steam and energy requirement in calcium looping conditions. *Appl. Energy* **2017**, *206*, 869–878. [CrossRef]
58. Wu, Z.H.; Kou, P.; Yu, Z.W. The modulation of desulphurization properties of calcium oxide by alkali carbonates. *J. Therm. Anal. Calorim.* **2002**, *67*, 745–750. [CrossRef]
59. Wieczorek-Ciurowa, K. Peculiarities of interactions in the $CaCO_3$/CaO-SO_2/SO_3-air system a review. *J. Therm. Anal. Calorim.* **1998**, *53*, 649–658. [CrossRef]
60. Chen, X.; Zheng, Y.; Zheng, C.; Zhao, H. Research on the carbonation reaction of CaO. *J. Huazhong Univ. Sci. Techno. Nat. Sci. Ed.* **2003**, *31*, 54–55.
61. Szekely, J.; Evans, J.W.; Sohn, H.Y. *Gas-Solid Reactions*; Academic Press Inc.: London, UK, 1976.
62. Hughes, R.W.; Lu, D.; Anthony, E.J.; Wu, Y. Improved long-term conversion of limestone-derived sorbents for in situ capture of CO_2 in a fluidized bed combustor. *Ind. Eng. Chem. Res.* **2004**, *43*, 5529–5539. [CrossRef]